water

Article

Spatiotemporal Variation and Influence Factors of Vegetation Cover in the Yellow River Basin (1982–2021) Based on GIMMS NDVI and MOD13A1

Yi Cheng [1,2,3], Lijuan Zhang [4,*], Zhiqiang Zhang [2,3,5], Xueyin Li [6], Haiying Wang [7] and Xu Xi [8,*]

1 Institute of Surveying and Mapping, Information Engineering University, Zhengzhou 450046, China
2 Collaborative Innovation Center of Geo-Information Technology for Smart Central Plains, Zhengzhou 450046, China
3 Key Laboratory of Spatiotemporal Perception and Intelligent Processing, Ministry of Natural Resources, Zhengzhou 450046, China
4 College of Electrical Engineering and Automation, Luoyang Institute of Science and Technology, Luoyang 471023, China
5 College of Surveying and Geo-Informatics, North China University of Water Resources and Electric Power, Zhengzhou 450046, China
6 College of Earth and Planetary Sciences, University of Chinese Academy of Sciences, Beijing 100049, China
7 Key Laboratory of Geospatial Technology for Middle and Lower Yellow River Regions, Henan University, Ministry of Education, Kaifeng 475000, China
8 School of Geography Science and Geomatics Engineering, Suzhou University of Science and Technology, Suzhou 215009, China
* Correspondence: ly_zlj8@163.com (L.Z.); xixu2013@163.com (X.X.)

Citation: Cheng, Y.; Zhang, L.; Zhang, Z.; Li, X.; Wang, H.; Xi, X. Spatiotemporal Variation and Influence Factors of Vegetation Cover in the Yellow River Basin (1982–2021) Based on GIMMS NDVI and MOD13A1. *Water* **2022**, *14*, 3274. https://doi.org/10.3390/w14203274

Academic Editor: Salvador García-Ayllón Veintimilla

Received: 30 August 2022
Accepted: 11 October 2022
Published: 17 October 2022

Abstract: Depicting the spatiotemporal dynamics of vegetation cover in the Yellow River Basin (YRB) and delineating the influences of climate change and human activities on the dynamics have been of significant importance for understanding the surface earth systems in general and also for formulating ecological protection plans of the YRB in particular. This study uses the GIMMS NDVI dataset from 1982 to 2015 and the MOD13A1 NDVI dataset from 2000 to 2021 to explore the spatial and temporal characteristics of vegetation cover in the YRB for the period from 1982 to 2021 with an attempt to reveal the influencing factors. The spatial distribution and temporal variation characteristics of vegetation cover are analyzed by maximum value composite, Theil-Sen median trend analysis, and Mann–Kendall test. Combined with the mean annual temperature and annual precipitation in the same period, influencing factors of vegetation cover in the YRB are discussed by using binary linear regression analysis and residual analysis. Results show that: (1) the multi-year average NDVI values increase from the northwest to the southeast and that the annual mean values of the vegetation covers fluctuate relatively greatly along an increasing trend with a growth rate of 0.019/(10a). Understandably, the monthly mean NDVI values show a single-peak distribution pattern, with August being the peak time (0.4936). (2) 77.35% of the studied areas are characterized by exhibiting an increasing trend of vegetation cover during the study period (i.e., 1982–2021). (3) Vegetation cover of the YRB is affected by the combined effects of climate change and human activities, with human activities being more significant in the observed amelioration of vegetation cover.

Keywords: vegetation cover; GIMMS NDVI; MOD13A3; residual analysis; Yellow River Basin (YRB)

1. Introduction

Vegetation is a crucial component of terrestrial ecosystems and plays an important role in terrestrial carbon balance and climate regulation [1–4]. The study on the dynamic change [5–7], driving mechanism [8,9], and regulation of vegetation ecosystem [10,11] under changing environment is one of the core contents of global change research. Monitoring the vegetation dynamics and quantifying the impact of climate change and human activities on vegetation dynamics have important practical value for determining ecological engineering layout and management countermeasures and have become a research hotspot of sustainable management of vegetation ecosystems under the changing environment [4,7,12,13].

Normalized difference vegetation index (NDVI) is a commonly used remote sensing index to reflect vegetation dynamics [14–16]. With the rapid development of geographic information technology, a large number of NDVI products have been produced. AVHRR NDVI [17,18], SPOT VGT NDVI [19], and MODIS NDVI [3,20] are widely used global NDVI products. GIMMS NDVI 3 g dataset is based on the AVHRR sensor. The product covers the period from January 1982 to December 2015, with a spatial resolution of 8 km and a time resolution of 15 days [18,21,22]. It is the NDVI product with the longest time series so far. SPOT VGT NDVI product covers the period from April 1998 to the present, with a temporal resolution of 10 days and a spatial resolution of 1 km [19]. MODIS NDVI includes four NDVI products, namely, MOD13Q1, MOD13A1, MOD13A2, and MOD13A3. Their spatial resolutions are 250 m, 500 m, and 1 km, respectively, and their temporal resolutions are all 16 days [23–26]. The time series and spatial resolution of different products are also different, which can describe the spatiotemporal characteristics of vegetation coverage at different scales in different time periods [18,19,23].

In recent years, a large number of scholars have carried out spatiotemporal variation and influence factors of vegetation cover based on the products mentioned above in different research areas [27–30]. Gu et al. explored the vegetation changes and influencing factors in the Red River basin from 2000 to 2014 based on MOD13Q1 NDVI data [31]. The results show that both precipitation and temperature have time lag effects on vegetation change, precipitation has a greater impact on vegetation change than temperature, and the Grain for Green Project affects the temporal and spatial patterns of vegetation coverage. Gao et al. found that the annual and interannual NDVI changes in Mu Us sandy land are dominated by temperature and precipitation, respectively, and the impact of human activities on vegetation improvement in Mu Us sandy land is greater than in climate change [32]. Taking the North China Plain as a study area, Duo et al. have carried out relevant studies and found that the effect of human activities in the vegetation degradation region is higher than that in the improvement region. However, after the climate abruptly changes, the conclusion is just the opposite [1]. Zhang et al. found that vegetation improvement is mainly driven by climate change, and human activities have an inhibitory effect on vegetation growth in the Three-River headwaters region [33]. In general, the characteristics and influence factors of vegetation cover change in different regions are quite different [19,31,33].

The Yellow River, the second longest river in China and often named “the mother river of the Chinese nation”, plays an important role in China’s economic and social development and ecological security [34,35]. Due to the combined action of precipitation, evaporation, topography, and human activities, the ecological environment of the Yellow River Basin (YRB) is fragile; meanwhile, water and soil loss is serious [36]. The YRB is the most important region of water and soil loss in China and even in the world, and the area of soil and water loss region accounts for 62% of the total area of the YRB [35,36]. The ecological protection and high-quality development of the YRB have become a major national strategy in China [37]. Understanding the vegetation dynamics and its response to climate change and human activities in the YRB is of great application value for formulating reasonable ecological protection schemes. However, previous studies have often selected local regions of the YRB (such as the source region of the Yellow River, the Loess Plateau, and the Yellow River Delta, etc.), and the time span is mostly before 2015 at the scale of 8 km [5,11,16].

Based on the above background, this study takes the whole YRB as the study area and researches the vegetation variation and its influence factors. The aims of this study are to (1) assess the spatial pattern and interannual variation of vegetation cover in the YRB over the period of 1982–2021 and (2) examine the influence factors of vegetation cover change in the YRB.

2. Study Area and Datasets

2.1. Study Area

The YRB (95°53′–119°12′ E, 32°9′–41°50′ N) includes parts of nine provinces, as Figure 1 shows, and its total area is approximately 790,000 km^2 [38]. Qinghai province, the birthplace of the Yellow River, has the largest area in the YRB, accounting for 19% of the total area of the YRB. Shandong Province, the estuary of the Yellow River, has the smallest area in the basin, accounting for only 1.72%. The terrain of the YRB is high in the west and low in the east [39,40]. The western region is composed of a large number of high-altitude mountains (such as the Bayan Har Mountains and Qilian Mountains) with an average elevation of higher than 4000 m, and its vegetation types are mainly forest and grassland [3]. The central region (altitude between 1000 and 2000 m) belongs to the Loess Plateau with serious water and soil loss, and its vegetation types are mainly woodland, grassland, and farmland. It should be emphasized that since 1999, the Chinese government has carried out a series of ecological restoration projects in this region, including the Grain for Green Program and the Natural Forest Conservation Program, which has significantly improved the region's ecological environment [41,42]. The eastern region is mainly composed of the alluvial plain of the Yellow River, and its elevation is less than 100 m. Most areas of the YRB belong to arid and semi-arid climates, and water resources are in congenital shortage with an average annual precipitation of 470 mm [39]. The annual precipitation in the YRB increases in a fluctuating manner with change rates of 1.662 mm/decade from 1982 to 2015 and the average annual temperature range between 4.3 and 14.3 °C.

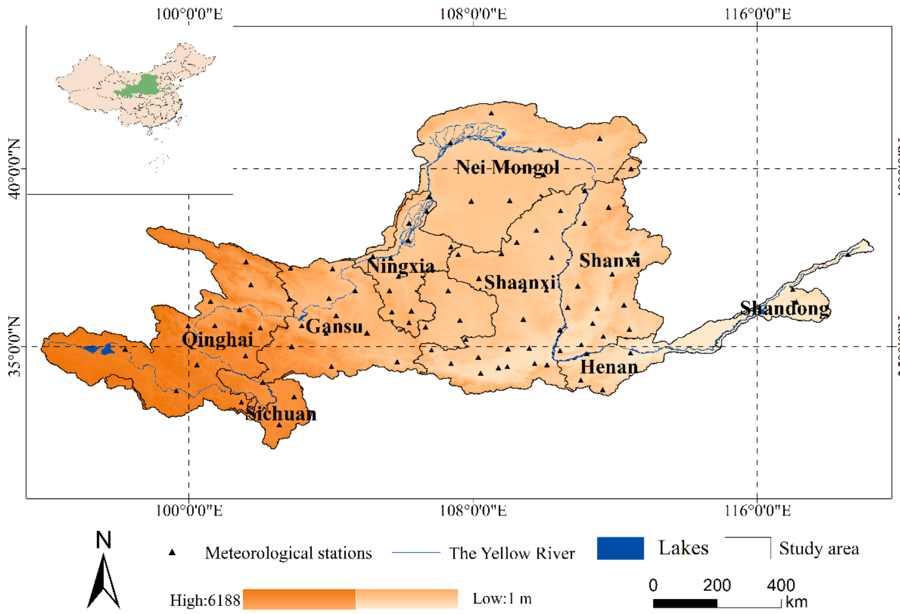

Figure 1. Digital elevation model, meteorological stations, and administrative divisions of the YRB.

2.2. Datasets

The datasets used in this study mainly include the GIMMS NDVI 3 g, MOD13A3 NDVI, and meteorological dataset. The GIMMS NDVI 3 g dataset, released by the Global Monitoring and Modeling Research Group (GIMMS) of the National Oceanic and Atmospheric Administration (NOAA), is a global NDVI vegetation index product with a spatial resolution of 8 km and a 15-day temporal resolution [18]. Compared with other commonly used global NDVI vegetation index products, The GIMMS NDVI 3 g dataset has the longest time series despite its low spatial resolution, so it can better reflect the long-term temporal characteristics of vegetation cover changes. The MOD13A3 NDVI dataset is a 1 km resolution vegetation index product with 16-day temporal resolution from MODIS remote sensing image [43].

The meteorological dataset, including daily temperature and precipitation data of 126 meteorological stations in the YRB and its surrounding areas, is acquired from the National Meteorological Science Data Center of China (https://data.cma.cn/ (accessed on 13 April 2021)).

3. Methodology

Figure 2 shows the flowchart of this study, which mainly consists of the following four steps: (1) dataset preprocessing, including the NDVI dataset and the meteorological dataset; (2) data fusion, establishing a unary linear regression model and producing 8 km spatial resolution NDVI dataset of the YRB from 1982 to 2021; (3) spatiotemporal dynamic analysis, analyzing the spatial pattern and temporal change characteristics of vegetation cover in the YRB; (3) influence factors analysis, exploring the key driving forces affecting vegetation cover change.

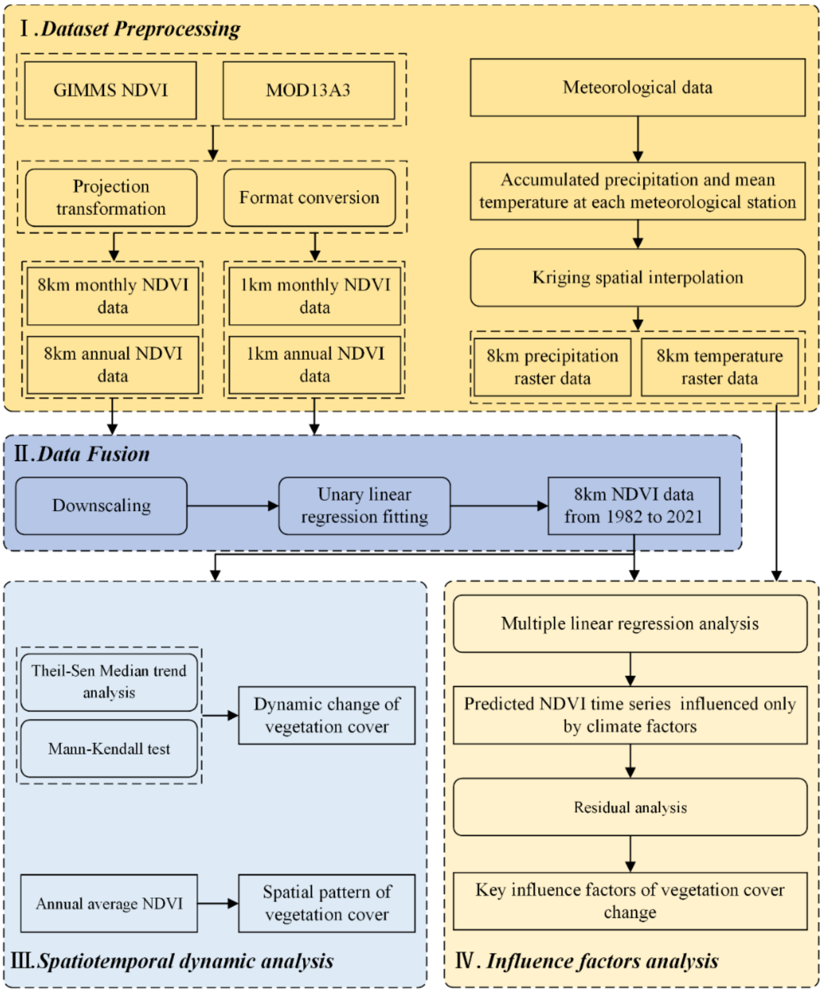

Figure 2. The flowchart of this study.

3.1. Dataset Preprocessing

A series of preprocessing is performed on the GIMMS NDVI dataset and MOD13A3 NDVI dataset in this study, including projection transformation, format conversion, maximum value composite (MVC), and average calculation. This projection of the datasets is first defined as WGS84_Albers with the main parameters set as follows: central meridian is set to 115.0, and two standard parallels are set to 25.0 and 47.0, respectively. Then, monthly NDVI datasets are obtained using the MVC method to eliminate the influences of clouds, atmosphere, and solar altitude angle. Finally, the annual NDVI datasets are obtained by average calculation of monthly NDVI datasets of the growing season (April–October).

The meteorological datasets are also carried out through a series of preprocessing in this study. The cumulative precipitation and average temperature of each meteorological station from March to October are firstly calculated. Previous studies [19] have indicated that precipitation and temperature have hysteresis effects on vegetation change; thus, cumulative precipitation and average temperature from March to October are calculated in this study to analyze the response of vegetation cover to climate change and human activities. The ordinary Kriging interpolation method is then used to obtain the spatially interpolated raster data of the cumulative precipitation and average temperature year by year with a grid size of 8 km. The first and second rows in Figure 3 show the spatially interpolated raster data and the accuracy of the cumulative precipitation and average temperature in 2015, and the squared correlation coefficients between the measured and interpolated values of these two raster data are 0.675 and 0.640, respectively, which is calculated by the cross-validation method.

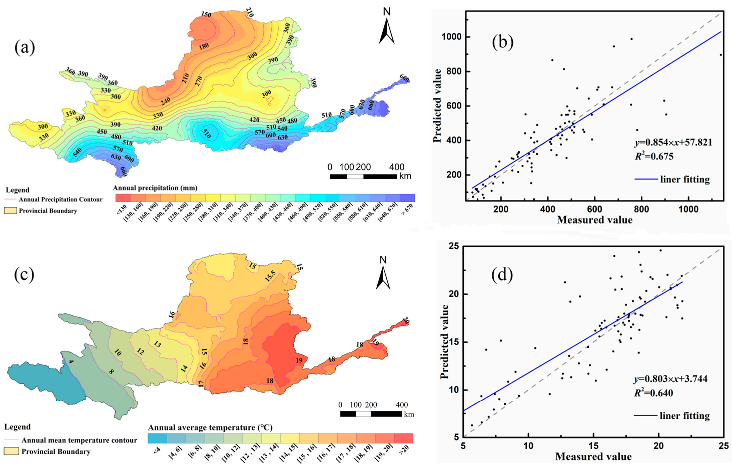

Figure 3. The spatially interpolated raster data and accuracy of cumulative precipitation and average temperature in 2015. (**a**,**b**) are the spatially interpolated raster data and accuracy of cumulative precipitation, respectively. (**c**,**d**) are the spatially interpolated raster data and accuracy of average temperature, respectively.

3.2. Data Fusion

This study focus on exploring the spatiotemporal variation characteristics of vegetation cover in the YRB at the 8 km scale. Therefore, the GIMMS NDVI dataset and MOD13A3 NDVI dataset are fused to generate an 8 km scale vegetation cover dataset in the YRB from 1982 to 2021. Specific methods and procedures are as follows:

(1) Resampling MOD13A3 NDVI. The bilinear interpolation method is used to resample MOD13A3 NDVI in the YRB from 2000 to 2021 to 8 km;

(2) Establishing a consistency correction model. The spectral resolution of different sensors is different. In order to maintain the consistency of the NDVI dataset generated by data fusion [19], the resampled MOD13A3 NDVI should be corrected. Previous studies have shown that NDVI from different sensors has a certain linear correlation [19]. Therefore, this study intends to establish a unary linear regression model pixel by pixel to correct the resampled MOD13A3 NDVI based on the resampled MOD13A3 NDVI and GIMMS NDVI from 2000 to 2015. The model is as follows:

$$NDVI_{MC(i,d)} = k \times NDVI_{M(i,d)} + b \quad (1)$$

where $NDVI_{MC(i,d)}$ and $NDVI_{M(i,d)}$ represent the NDVI values with pixel i year d of the corrected MOD13A3 NDVI resampling data and resampled MOD13A3 data, respectively.

k and b represent the slope and intercept of the model, respectively, which are estimated using GIMMS NDVI and resampled MOD13A3 NDVI from 2000 to 2015.

Figure 4 shows the correlation between measured (GIMMS NDVI) and predicted (corrected MOD13A3 NDVI resampling data, $NDVI_{MC(i,d)}$) values, which are made using 2242 randomly selected sample points from 2000 to 2015. It is not difficult to find that the NDVI data (i.e., predicted NDVI) corrected by the linear regression model and GIMMS NDVI data (i.e., measured NDVI) have suitable consistency (R^2 = 0.987).

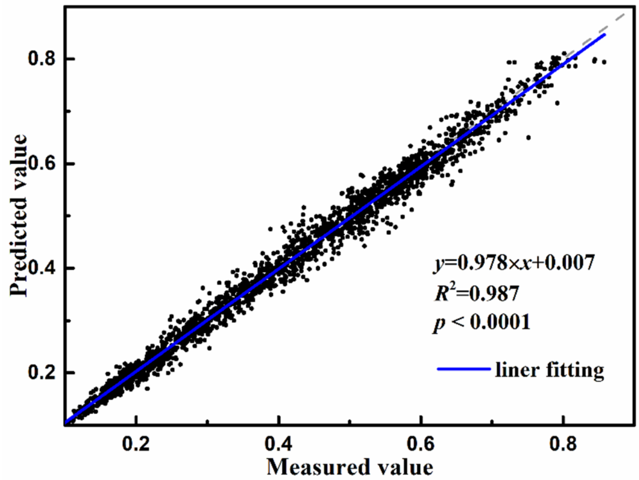

Figure 4. Correlation between measured (GIMMS NDVI) and predicted (corrected MOD13A3 NDVI resampling data) values.

(3) Establishing an 8 km scale NDVI dataset for the YRB from 1982 to 2021. The above model is used to correct the resampling MOD13A3 NDVI data from 2016 to 2021 and then combined with GIMMS NDVI data from 1982 to 2015 to generate an 8 km scale NDVI dataset of the YRB from 1982 to 2021.

3.3. Spatiotemporal Dynamic Analysis

In this study, the Theil-Sen median trend analysis method (TSM) is used to analyze the change trend of vegetation cover in the YRB during 1982–2015, and the Mann–Kendall test method (MK) is used to test the significance of the change trend. The TSM is a robust non-parametric statistical trend analysis method, which can effectively reduce the interference of abnormal values [3,44,45]. It is calculated by:

$$S_{NDVI} = \text{median}\left(\frac{NDVI_j - NDVI_i}{j - i}\right),\ 1982 \leq i < j \leq 2015 \tag{2}$$

where $NDVI_j$ and $NDVI_i$ represent the NDVI values with years i and year j, respectively. S_{NDVI} is the median of n $(n-1)/2$ combinations and reflects the change trend of vegetation cover. When $S_{NDVI} > 0$, the vegetation cover shows an increasing trend and vice versa.

The MK is a non-parametric statistical test method used to test whether the trend of change is significant. The MK has the advantage that samples do not need to obey certain distributions and has a strong ability to resist outliers [3,44]. The calculation formula is as follows:

$$Z = \begin{cases} \frac{S-1}{\sqrt{\text{var}(S)}} & S > 0 \\ 0 & S = 0 \\ \frac{S+1}{\sqrt{\text{var}(S)}} & S < 0 \end{cases} \tag{3}$$

where

$$S = \sum_{i}^{n-1} \sum_{j=i+1}^{n} \text{sign}(NDVI_j - NDVI_i) \quad (4)$$

$$\text{sign}(NDVI_j - NDVI_i) = \begin{cases} 1 & NDVI_j - NDVI_i > 0 \\ 0 & NDVI_j - NDVI_i = 0 \\ -1 & NDVI_j - NDVI_i < 0 \end{cases} \quad (5)$$

$$\text{var}(s) = \frac{n \times (n-1)(2n+5)}{18} \quad (6)$$

where n represents the number of years in the study period, and it is equal to 34 in this study. sign() is a symbol function. Z represents a statistic from a standardized normal distribution with a range of $(-\infty, +\infty)$. For a given significance level α, $|Z| > \mu_{1-\alpha/2}$ represents the change trend is significant in the level α. Confidence levels of 95% and 99% are used. According to the S_{NDVI} and $|Z|$, the change trend of vegetation cover is divided into five categories, as shown in Table 1.

Table 1. Classification of vegetation cover change trend in the YRB.

Classification Criterion	Vegetation Cover Change Trend
$S_{NDVI} > 0$ and $\lvert Z \rvert \geq 2.58$	Significant improvement
$S_{NDVI} > 0$ and $1.96 \leq \lvert Z \rvert < 2.58$	Slight improvement
$\lvert Z \rvert < 1.96$	No significant change
$S_{NDVI} \leq 0$ and $1.96 \leq \lvert Z \rvert < 2.58$	Slight degradation
$S_{NDVI} \leq 0$ and $\lvert Z \rvert \geq 2.58$	Significant degradation

3.4. Influence Factors Analysis

Residual analysis is a widely used method to analyze the influence factors of vegetation cover change [16,46]. The difficulty of the method is to accurately predict NDVI value only affected by climate change. Since 2000, a series of ecological restoration programs (such as the afforestation project and the Grain for Green Program, etc.) have been implemented, and vegetation cover is significantly improved in the YRB. Compared with the study period after 2000, the impact of human activities on vegetation cover change during 1982–2000 is weak. Therefore, this study assumed that vegetation cover change during 1982–2000 is only determined by climate change. Based on the assumptions, this study uses annual NDVI as the dependent variable and average temperature and cumulative precipitation from March to October as independent variables to construct a bivariate linear regression model per pixel to predict the NDVI value only affected by climate change and explore the key driving forces affecting vegetation cover change. Specific steps are as follows.

(1) Building the bivariate linear regression model per pixel and predicting NDVI value ($NDVI_{CC}$) only affected by climate change.

$$NDVI_{CC} = a \times Tem + b \times Pre + c \quad (7)$$

where *Tem* and *Pre* represent the average temperature and cumulative precipitation pre pixels from March to October, respectively. a, b, and c represent the model parameters, which are obtained by least square fitting using data from 1982 to 2000.

(2) Predicting NDVI value ($NDVI_{HA}$) affected by human activities.

$$NDVI_{HA} = NDVI - NDVI_{CC} \quad (8)$$

where NDVI indicates the annual NDVI value of each pixel.

(3) Exploring the influencing factors of vegetation cover change.

Firstly, the unary linear regression analysis method is used to calculate the slope of the trend line of the interannual variation of $NDVI$, $NDVI_{CC,}$ and $NDVI_{HA}$ pixel by pixel. The calculation model is as follows:

$$slope_A = \frac{n \times \sum_{i=1}^{n} (i \times A_i) - \sum_{i=1}^{n} i \times \sum_{i=1}^{n} A_i}{n \times \sum_{i}^{n} i^2 - \left(\sum_{i}^{n} i\right)^2} \quad (9)$$

where $slope_A$ represents the slope of the trend line of data series A. When A is NDVI, $NDVI_{CC,}$ and $NDVI_{HA}$ data series, the slope of the trend line is $slope_{NDVI}$, $slope_{NDVI_{CC}}$ and $slope_{NDVI_{HA}}$, respectively. N represents the annual span in the study period, and this study analyzes the influencing factors of vegetation cover change from 2000 to 2021, so n is set to 22. According to $slope_{NDVI}$, $slope_{NDVI_{CC}}$, and $slope_{NDVI_{HA}}$, the influencing factors of vegetation cover change in the YRB are divided into six categories, as shown in Table 2.

Table 2. Identification criterion of the drivers of NDVI change.

$slope_{NDVI}$	Identification Criterion [16]		Influence Factors
	$slope_{NDVI_{CC}}$	$slope_{NDVI_{HA}}$	
>0	>0	>0	Synergy boost
	>0	<0	Climate change boost
	<0	>0	Human activities boost
<0	<0	<0	Synergy inhibition
	<0	>0	Climate change inhibition
	>0	<0	Human activities inhibition

Note: CC and HA stand for climate change and human activity, respectively.

4. Results

4.1. Spatial Pattern of Vegetation Cover in the YRB

According to multi-year average NDVI, vegetation cover types in the YRB have five categories, LVC [0.0–0.2), RLVC [0.2–0.4), MVC [0.4–0.6), RHVC [0.6–0.8), and HVC [0.8–1.0). Figure 5 shows the spatial pattern of vegetation cover in the YRB, and Table 3 shows the statistical results of the area occupied by different vegetation cover types in the hydrological units (SRYRB, URYRB, MAYRB, and DRYRB represent the source region, the upper, middle and downstream regions of the Yellow River, respectively). It is not difficult to find that: (1) vegetation cover in the YRB is obvious spatial heterogeneity, showing an increasing spatial pattern from northwest to southeast. (2) LVC and RLVC mainly distribute in the URYRB, the SRYRB, and the northwest of MAYRB, accounting for 49.29% of the YRB. (3) RLVC and MVC are the main vegetation cover types in the YRB, accounting for 71.32% of the YRB, mainly distributed in the URYRB and MAYRB. (4) HVC distribute in patches in the southeast of the SRYRB, the southeast of the MAYRB, and the southwest of the DRYRB, accounting for 14.85% of the total basin.

Table 3. Statistics of area occupied by different vegetation cover types in the YRB.

	Occupies the Area of Total YRB	LVC	RLVC	MVC	RHVC	HVC
YRB	100%	13.44%	35.85%	35.47%	14.85%	0.38%
SRYRB	16.14%	5.35%	30.91%	46.09%	17.65%	0.00%
URYRB	38.04%	32.39%	42.14%	20.78%	4.69%	0.00%
MAYRB	42.96%	0.60%	36.01%	42.20%	20.53%	0.66%
DRYRB	2.86%	0.00%	0.30%	64.35%	35.35%	0.00%

Notes: YRB, SRYRB, URYRB, MAYRB, and DRYRB represent the Yellow River Basin, the source region, and the upper, middle, and downstream regions of the Yellow River, respectively. LVC, RLVC, MVC, RHVC, and HVC stand for low vegetation cover type, relatively low vegetation cover type, medium vegetation cover type, relatively high vegetation cover type, and high vegetation cover type, respectively.

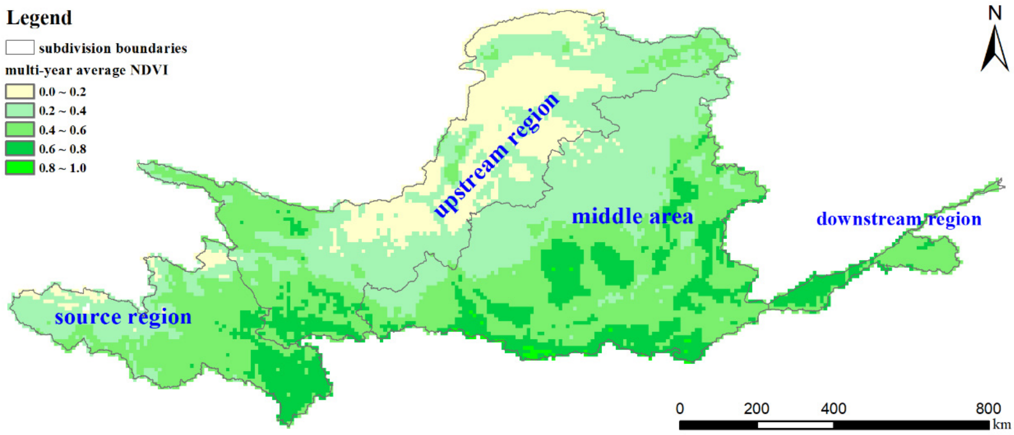

Figure 5. Spatial pattern of vegetation cover in the YRB.

4.2. Temporal Variation Characteristics of Vegetation Cover in the YRB

Figure 6a shows the temporal variation characteristics of monthly NDVI in the YRB. The monthly NDVI is obtained by averaging the corresponding monthly NDVI from 1982 to 2021. Figure 6b–f show the temporal variation characteristics and unary linear fitting lines of NDVI in the YRB, the source region (SRYRB), the upper (URYRB), middle (MAYRB), and downstream regions (DRYRB) of the YRB, respectively. It is not difficult to find that: (1) the monthly mean NDVI value of vegetation cover in the YRB during 1982–2021 shows a change process of first increasing and then decreasing, and the monthly mean NDVI value in August is the largest (0.4936) (Figure 6a). (2) In the past 40 years, the vegetation cover in the YRB has shown an annual increase with a growth rate of 0.019/10a (Figure 6b). (3) The vegetation cover of the MAYRB has the fastest growth rate (0.030/10a), while the vegetation cover in the SRYRB has a smaller growth range, with a growth rate of 0.006/10a. (4) On the annual mean NDVI value, the vegetation cover in the LRYRB is the best, followed by the MAYRB and the SRYRB, and the vegetation cover in the URYRB is the worst.

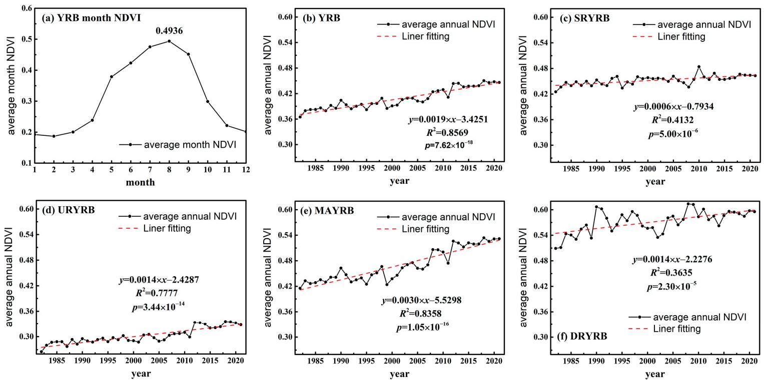

Figure 6. Temporal variation characteristics of vegetation cover in the YRB and its subregions (SRYRB, URYRB, MAYRB, and DRYRB represent the source region, the upper, middle, and downstream regions of the Yellow River, respectively).

Figure 7 shows the spatial distribution characteristics of vegetation cover change trend in the YRB. Table 4 shows the statistical results of the area occupied by vegetation cover change trend in the YRB and different water resources zones. It shows that: (1) vegetation cover in most regions of the YRB shows a significant improvement trend in the past 40 years, and the area of significant improvement trend accounts for 62.33% of the total basin. The vegetation cover degradation area and no significant change area are mainly distributed in the SRYRB, the urban concentrated development area of the northwest of the URYRB, and the west of the MAYRB, accounting for 22.65% of the total area. (2) The vegetation cover change types in the SRYRB are complex and diverse. Except for urban concentrated development areas (e.g., The Guanzhong Plains Urban Agglomeration and Central Plains Urban Agglomeration), the vegetation cover in most of the MAYRB shows a significant improvement trend, which may be related to the positive effects of China's projects (e.g., the conversion of farmland to forest (grassland)) and the implementation of ecological management policies.

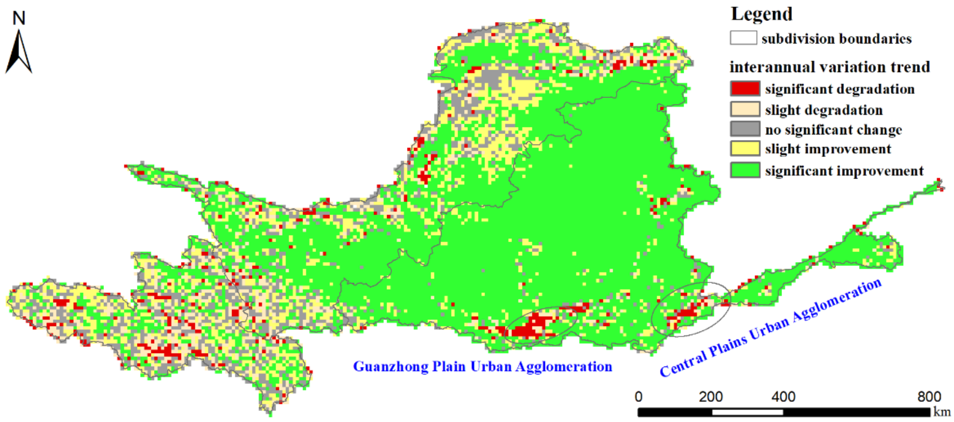

Figure 7. Spatial distribution characteristics of vegetation cover change trends in the YRB.

Table 4. Statistic of area occupied by vegetation cover change trend in the YRB and different water resources zones.

	SID	SLD	NSC	SLM	SIM
YRB	2.51%	5.74%	14.40%	15.02%	62.33%
SRYRB	0.88%	2.51%	5.35%	4.17%	3.47%
URYRB	0.76%	2.43%	7.41%	8.32%	19.31%
MAYRB	0.83%	0.69%	1.48%	2.30%	37.19%
DRYRB	0.05%	0.12%	0.15%	0.23%	2.36%

Notes: SID, SLD, NSC, SLM, and SIM represent significant degradation, slight degradation, no significant change, slight improvement, and significant improvement, respectively.

4.3. Influence Factors of Vegetation Cover Change in the YRB

Referring to the classification criteria [16] of influence factors of vegetation cover change, this study first analyzes the impacts of climate change and human activities on vegetation cover restoration one by one (Figure 8). According to Figure 8a and Table 5, the areas with basically no impact of climate change on vegetation cover restoration are mainly distributed in Gansu Province, Ningxia Hui Autonomous Region, and part of Shaanxi Province, accounting for 27.41% of the total basin. The boost effect mainly concentrated in the eastern of Qinghai Province, Henan Province, Shanxi Province, and Qilian Mountains, accounting for 42.39%. The inhibition areas are mainly in the SRYRB, Ordos Plateau, Mu Us sandy land, and central Shanxi Province, accounting for 30.19%. The areas of significant inhibition and moderate inhibition are about 6.84%, which are mainly distributed in the central region of Shanxi Province and part of the Inner Mongolia Autonomous Region. The main reason may be that the precipitation in these regions is small (the cumulative precipitation from March to October is less than 350 mm, Figure 2), and the temperature is high, which results in large evaporation.

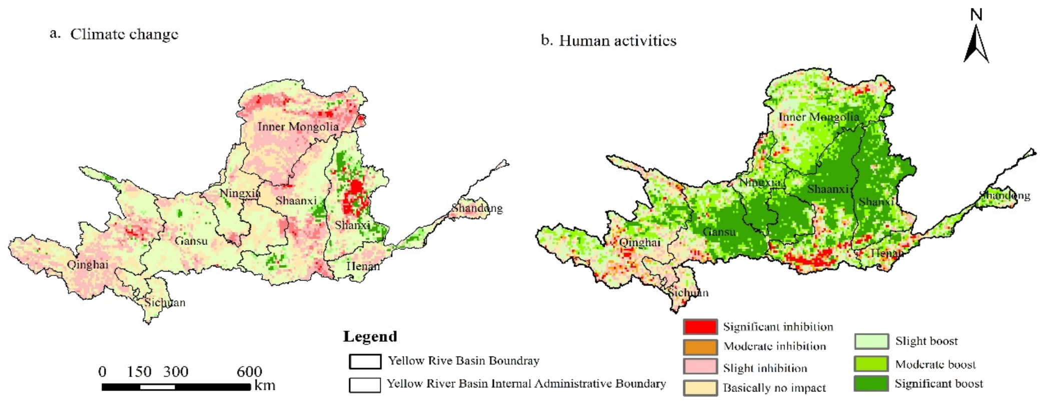

Figure 8. Spatial distribution of climate change (**a**) and human activities (**b**) impacts on vegetation restoration in the YRB during 2001–2021.

Table 5. The impacts of climate change and human activities on vegetation restoration in the YRB.

	Significant Inhibition <−2.0	Moderate Inhibition −2.0~−1.0	Slight Inhibition −1.0~−0.2	Basically No Impact −0.2~0.2	Slight Boost 0.2~1.0	Moderate Boost 1.0~2.0	Significant Boost ≥2.0
Climate change(%)	0.93	5.91	23.35	27.43	35.51	5.09	1.78
Human activities(%)	2.57	7.49	3.15	13.09	21.19	15.31	37.19

According to Figure 8b and Table 5, the areas where human activities have little impact on vegetation cover restoration are mainly distributed in the URYRB with 13.09%. The area of its boost effect accounts for 73.69%, among which 52.50% are significant and moderate boost effects, mainly concentrated in the MAYRB. The inhibitory effect is mainly distributed in the SRYRB, Ningxia plain region, southern Shaanxi Province, and so on, accounting for 13.21%, and 10.06% of them have a significant and moderate inhibitory effect.

In the study period, the average impacts of climate change and human activities on vegetation cover change in the YRB are -0.12×10^{-3} a^{-1} and 2.83×10^{-3} a^{-1}, respectively, indicating that the impact of human activities on vegetation cover change in the YRB is mainly promoted.

Figure 9 shows the impacts of climate change and human activities on vegetation cover change in the YRB. The results (Figure 9 and Table 6) show that about 36.65% of the areas are affected by the synergy of climate change and human activities, which are mainly distributed in the eastern Gansu Province, northern Shaanxi Province, Shanxi Province, and DRYRB. About 2.19% of the areas affected only by climate change have a positive effect on vegetation restoration, affected only by human activities, about 46.13%. About 7.32% of vegetation restoration is inhibited by climate change and human activities, mainly in the ARYRB. The area that is only affected by climate change and has an inhibitory effect on vegetation restoration accounted for 2.53%, and human activities are 5.18%, mainly distributed in the southern edge of the YRB.

Table 6. Statistics of the influence factors of vegetation cover changes in the YRB during 2001–2021.

Influence Factors	Synergy Boost	CC Boost	HA Boost	Synergy Inhibition	CC Inhibition	HA Inhibition
Ratio(%)	36.65	2.19	46.13	7.32	2.53	5.18

Note: CC and HA stand for climate change and human activity, respectively.

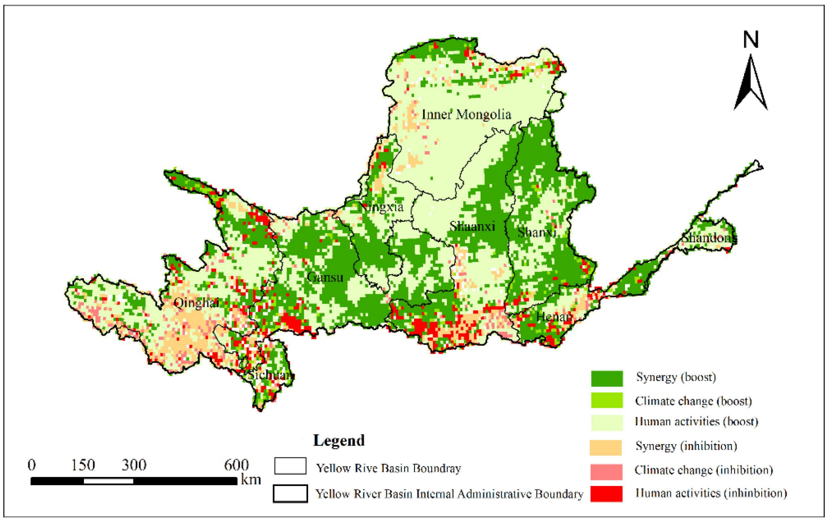

Figure 9. Spatial distribution of the influence factors of vegetation cover changes in the YRB during 2001–2021.

5. Discussion

In this study, vegetation cover change characteristics over longer time periods are analyzed by fusing the GIMMS NDVI dataset and MOD13A1 NDVI dataset. The results show that (1) the temporal variation characteristic of vegetation cover in the YRB has obvious spatial heterogeneity, and the overall trend is fluctuating upward. (2) Vegetation cover increases gradually from northwest to southeast. These results are basically consistent with the conclusions of previous studies [46,47]. Compared with the annual growth rate of vegetation cover in different periods, the rate during 1982–2021 (0.019/10a) is slightly higher than that during 1982–2015 (0.015/10a), indicating that the growth rate of vegetation cover increase during 2016–2021.

Human activities have both positive and negative effects on vegetation cover restoration [23,27]. For example, urban construction and reservoir storage lead to the change of land use type from forest, grassland, and farmland to impervious surface or water. Overload herds cause large areas of grass to be eaten. All of these human activities have resulted in the reduction in vegetation cover. In addition, ecological protection measures such as afforestation and animal husbandry control have increased vegetation cover area. Vegetation cover has been significantly improved in the Loess Plateau with the implementation of a series of ecological protection policies, such as afforestation and returning farmland to forest. In general, this study concludes that the positive effects of human activities in the YRB are greater than the negative effects, indicating that a series of ecological protection policies in the YRB is effective.

This study analyzes the key driving forces affecting vegetation cover change, which has important reference significance for formulating scientific and reasonable ecological and environmental protection measures in the YRB. However, this study still has the following two shortcomings: (1) lack of in-depth analysis of the influence mechanism of climate change factors (precipitation and temperature) on vegetation cover change. (2) Lack of detailed analysis of the impact of different human activities (such as population growth, urbanization, agricultural development, and ecological protection policies) on vegetation cover. Solving the above shortcomings will help to deeply understand the influencing mechanism of vegetation cover change in the YRB, which is the follow-up content of this study.

6. Conclusions

Based on the GIMMS NDVI dataset, MOD13A1 NDVI dataset, and meteorological dataset, this study analyzes the spatiotemporal variation and influencing factors of vegetation cover in the YRB from 1982 to 2021. The main conclusions are as follows:

(1) In terms of spatial distribution, the vegetation cover in the YRB shows obvious spatial heterogeneity, which gradually increased from northwest to southeast, and the vegetation cover in the upper reaches of the YRB is the worst. The monthly average NDVI increases first and then decreases, and the NDVI in August is the largest (0.4936), which may be mainly due to the high temperature and high precipitation in the YRB in August. The interannual variation showed a fluctuating growth trend, with an increase rate of 0.019/10a.

(2) The areas with significant improvement in vegetation cover account for 63% of the total basin. However, 22.65% of the basin show vegetation cover degradation or no significant change, which may be determined by the climatic characteristics of the YRB. The vegetation cover of most areas in the middle reaches of the YRB shows a significant improvement trend except for the urban concentrated development areas (such as the Guanzhong Plain Urban Agglomeration and the Central Plains Urban Agglomeration), which may be related to the positive effects of China's ecological management projects.

(3) The vegetation cover change in the YRB is influenced by both climate change and human activities. The areas in which human activities and climate change boosted vegetation cover restoration account for 46.13% and 2.19% of the total basin, respectively, indicating that human activities play a greater role in boosting vegetation cover restoration in the YRB.

Author Contributions: Conceptualization, Z.Z. and L.Z.; Data curation, L.Z. and H.W.; Formal analysis, L.Z. and H.W.; Funding acquisition, Y.C.; Methodology, Z.Z., X.L., and X.X.; Writing—original draft, Y.C. and X.L.; Writing—review and editing, Z.Z. and X.X. All authors have read and agreed to the published version of the manuscript.

Funding: This research was funded by the Joint Fund of Collaborative Innovation Center of Geo-Information Technology for Smart Central Plains, Henan Province, and Key Laboratory of Spatiotemporal Perception and Intelligent Processing, Ministry of Natural Resources (no. 212106), the Key Scientific Research Project of Henan Province (no. 22A170012), Key Science and Technology Research Project of Henan Province (no. 222102320236), Open Fund of Key Laboratory of Geospatial Technology for the Middle and Lower Yellow River Regions (Henan University), Ministry of Education (no. GTYR202106), and Natural Science Foundation of Henan (no. 202300410276).

Data Availability Statement: Not applicable.

Acknowledgments: The authors are grateful to the editors and the anonymous reviewers for their insightful comments and helpful suggestions.

Conflicts of Interest: The authors declare no conflict of interest.

References

1. Duo, A.; Zhao, W.; Qu, X.; Jing, R.; Xiong, K. Spatio-temporal variation of vegetation coverage and its response to climate change in North China plain in the last 33 years. *Int. J. Appl. Earth Obs.* **2016**, *53*, 103–117.
2. Gwapedza, D.; Hughes, D.A.; Slaughter, A.R.; Mantel, S.K. Temporal Influences of Vegetation Cover (C) Dynamism on MUSLE Sediment Yield Estimates: NDVI Evaluation. *Water* **2021**, *13*, 2707. [CrossRef]
3. Zhang, Z.Q.; Liu, H.; Zuo, Q.T.; Yu, J.T.; Li, Y. Spatiotemporal change of fractional vegetation cover in the Yellow River Basin during 2000—2019. *Resour Sci.* **2021**, *43*, 849–858.
4. Wu, D.; Zhao, X.; Liang, S.; Zhou, T.; Huang, K.; Tang, B.; Zhao, W. Time-lag effects of global vegetation responses to climate change. *Global Change Biol.* **2015**, *21*, 3520–3531. [CrossRef]
5. Cao, R.; Jiang, W.; Yuan, L.; Wang, W.; Lv, Z.; Chen, Z. Inter-annual variations in vegetation and their response to climatic factors in the upper catchments of the Yellow River from 2000 to 2010. *J. Geogr. Sci.* **2014**, *24*, 963–979. [CrossRef]

6. Liu, X.; Zhang, J.; Zhu, X.; Pan, Y.; Liu, Y.; Zhang, D.; Lin, Z. Spatiotemporal changes in vegetation coverage and its driving factors in the Three-River Headwaters Region during 2000–2011. *J. Geogr. Sci.* **2014**, *24*, 288–302. [CrossRef]
7. Liu, X.; Zhu, X.; Pan, Y.; Li, S.; Ma, Y.; Nie, J. Vegetation dynamics in Qinling-Daba Mountains in relation to climate factors between 2000 and 2014. *J. Geogr. Sci.* **2016**, *26*, 45–58. [CrossRef]
8. Shi, S.; Yu, J.; Wang, F.; Wang, P.; Zhang, Y.; Jin, K. Quantitative contributions of climate change and human activities to vegetation changes over multiple time scales on the Loess Plateau. *Sci. Total Environ.* **2021**, *755*, 142419. [CrossRef]
9. Zheng, K.; Wei, J.Z.; Pei, J.Y.; Cheng, H.; Zhang, X.L.; Huang, F.Q.; Li, F.M.; Ye, J.S. Impacts of climate change and human activities on grassland vegetation variation in the Chinese Loess Plateau. *Sci. Total Environ.* **2019**, *660*, 236–244. [CrossRef]
10. Zeng, Z.; Chen, A.; Piao, S.; Rabin, S.; Shen, Z. Environmental determinants of tropical forest and savanna distribution: A quantitative model evaluation and its implication. *J. Geophys. Res.-Biogeosci.* **2014**, *119*, 1432–1445. [CrossRef]
11. Wang, S.; Cui, C.; Dai, Q. Contributions of Vegetation Greening and Climate Change to Evapotranspiration Trend after Large-Scale Vegetation Restoration on the Loess Plateau, China. *Water* **2021**, *13*, 1755. [CrossRef]
12. Yuan, J.; Xu, Y.; Xiang, J.; Wu, L.; Wang, D. Spatiotemporal variation of vegetation coverage and its associated influence factor analysis in the Yangtze River Delta, eastern China. *Environ. Sci. Pollut. R.* **2019**, *26*, 32866–32879. [CrossRef]
13. Duan, L.; Liu, T.; Wang, X.; Luo, Y. Spatio-temporal patterns of water table and vegetation status of a deserted area. *Water* **2015**, *7*, 5788–5805. [CrossRef]
14. Martínez, B.; Gilabert, M.A. Vegetation dynamics from NDVI time series analysis using the wavelet transform. *Remote Sens. Environ.* **2009**, *113*, 1823–1842. [CrossRef]
15. Feng, D.; Wang, J.; Fu, M.; Liu, G.; Zhang, M.; Tang, R. Spatiotemporal variation and influencing factors of vegetation cover in the ecologically fragile areas of China from 2000 to 2015: A case study in Shaanxi Province. *Environ. Sci. Pollut. R.* **2019**, *26*, 28977–28992. [CrossRef]
16. Sun, W.; Song, X.; Mu, X.; Gao, P.; Wang, F.; Zhao, G. Spatiotemporal vegetation cover variations associated with climate change and ecological restoration in the Loess Plateau. *Agr. Forest Meteorol.* **2015**, *209*, 87–99. [CrossRef]
17. Kong, D.; Miao, C.; Borthwick, A.G.; Lei, X.; Li, H. Spatiotemporal variations in vegetation cover on the Loess Plateau, China, between 1982 and 2013: Possible causes and potential impacts. *Environ. Sci. Pollut. R.* **2018**, *25*, 13633–13644. [CrossRef]
18. Ibrahim, Y.Z.; Balzter, H.; Kaduk, J.; Tucker, C.J. Land degradation assessment using residual trend analysis of GIMMS NDVI3g, soil moisture and rainfall in Sub-Saharan West Africa from 1982 to 2012. *Remote Sens.* **2015**, *7*, 5471–5494. [CrossRef]
19. Xin, Z.B.; Xu, J.X.; Zheng, W. Spatiotemporal variations of vegetation cover on the Chinese Loess Plateau (1981–2006): Impacts of climate changes and human activities. *Sci China Ser. D* **2007**, *37*, 1504–1514. [CrossRef]
20. Chen, J.; Yan, F.; Lu, Q. Spatiotemporal variation of vegetation on the Qinghai–Tibet Plateau and the influence of climatic factors and human activities on vegetation trend (2000–2019). *Remote Sens.* **2020**, *12*, 3150. [CrossRef]
21. Jiang, S.; Chen, X.; Smettem, K.; Wang, T. Climate and land use influences on changing spatiotemporal patterns of mountain vegetation cover in southwest China. *Ecol. Indic.* **2021**, *121*, 107193. [CrossRef]
22. Tong, S.; Zhang, J.; Bao, Y. Spatial and temporal variations of vegetation cover and the relationships with climate factors in Inner Mongolia based on GIMMS NDVI3g data. *J. Arid Land* **2017**, *9*, 394–407. [CrossRef]
23. Huo, H.; Sun, C. Spatiotemporal variation and influencing factors of vegetation dynamics based on Geodetector: A case study of the northwestern Yunnan Plateau, China. *Ecol. Indic.* **2021**, *130*, 108005. [CrossRef]
24. Zhao, Y.; Feng, Q.; Lu, A. Spatiotemporal variation in vegetation coverage and its driving factors in the Guanzhong Basin, NW China. *Ecol. Inform.* **2021**, *64*, 101371. [CrossRef]
25. Nie, T.; Dong, G.; Jiang, X.; Lei, Y. Spatio-temporal changes and driving forces of vegetation coverage on the loess plateau of Northern Shaanxi. *Remote Sens.* **2021**, *13*, 613. [CrossRef]
26. Wang, H.; Xiao, W.; Zhao, Y.; Wang, Y.; Hou, B.; Zhou, Y.; Yang, H.; Zhang, X.; Cui, H. The spatiotemporal variability of evapotranspiration and its response to climate change and land use/land cover change in the three gorges reservoir. *Water* **2019**, *11*, 1739. [CrossRef]
27. Shi, P.; Hou, P.; Gao, J.; Wan, H.; Wang, Y.; Sun, C. Spatial-Temporal Variation Characteristics and Influencing Factors of Vegetation in the Yellow River Basin from 2000 to 2019. *Atmosphere* **2021**, *12*, 1576. [CrossRef]
28. Huang, S.; Zheng, X.; Ma, L.; Wang, H.; Huang, Q.; Leng, G.; Meng, E.; Guo, Y. Quantitative contribution of climate change and human activities to vegetation cover variations based on GA-SVM model. *J. Hydrol.* **2020**, *584*, 124687. [CrossRef]
29. Yang, C.; Fu, M.; Feng, D.; Sun, Y.; Zhai, G. Spatiotemporal changes in vegetation cover and its influencing factors in the loess Plateau of China based on the geographically weighted regression model. *Forests* **2021**, *12*, 673. [CrossRef]
30. Chen, W.; Bai, S.; Zhao, H.; Han, X.; Li, L. Spatiotemporal analysis and potential impact factors of vegetation variation in the karst region of Southwest China. *Environ. Sci. Pollut. R.* **2021**, *28*, 61258–61273. [CrossRef]
31. Gu, Z.; Duan, X.; Shi, Y.; Li, Y.; Pan, X. Spatiotemporal variation in vegetation coverage and its response to climatic factors in the Red River Basin, China. *Ecol. Indic.* **2018**, *93*, 54–64. [CrossRef]
32. Gao, W.; Zheng, C.; Liu, X.; Lu, Y.; Chen, Y.; Wei, Y.; Ma, Y. NDVI-based vegetation dynamics and their responses to climate change and human activities from 1982 to 2020: A case study in the Mu Us Sandy Land, China. *Ecol. Indic.* **2022**, *137*, 108745. [CrossRef]
33. Zhang, X.; Jin, X. Vegetation dynamics and responses to climate change and anthropogenic activities in the Three-River Headwaters Region, China. *Ecol. Indic.* **2021**, *131*, 108223. [CrossRef]

34. Bai, T.; Chang, J.X.; Chang, F.J.; Huang, Q.; Wang, Y.M.; Chen, G.S. Synergistic gains from the multi-objective optimal operation of cascade reservoirs in the Upper Yellow River basin. *J. Hydrol.* **2015**, *523*, 758–767. [CrossRef]
35. Bao, Z.; Zhang, J.; Wang, G.; Chen, Q.; Guan, T.; Yan, X.; Liu, C.; Liu, J.; Wang, J. The impact of climate variability and land use/cover change on the water balance in the Middle Yellow River Basin, China. *J. Hydrol.* **2019**, *577*, 123942. [CrossRef]
36. Zhang, X.; Liu, K.; Wang, S.; Wu, T.; Li, X.; Wang, J.; Wang, D.; Zhu, H.; Tan, C.; Ji, Y. Spatiotemporal evolution of ecological vulnerability in the Yellow River Basin under ecological restoration initiatives. *Ecol. Indic.* **2022**, *135*, 108586. [CrossRef]
37. Wu, Z.; Zhang, F.; Di, D.; Wang, H. Study of spatial distribution characteristics of river eco-environmental values based on emergy-GeoDa method. *Sci. Total Environ.* **2022**, *802*, 149679. [CrossRef]
38. Chen, Y.P.; Fu, B.J.; Zhao, Y.; Wang, K.B.; Zhao, M.M.; Ma, J.F.; Wu, J.H.; Xu, C.; Liu, W.G.; Wang, H. Sustainable development in the Yellow River Basin: Issues and strategies. *J. Clean Prod.* **2020**, *263*, 121223. [CrossRef]
39. Wang, S.Y.; Liu, J.S.; Ma, T.B. Dynamics and changes in spatial patterns of land use in Yellow River Basin, China. *Land Use Policy* **2010**, *27*, 313–323. [CrossRef]
40. Jiang, L.; Zuo, Q.; Ma, J.; Zhang, Z. Evaluation and prediction of the level of high-quality development: A case study of the Yellow River Basin, China. *Ecol. Indic.* **2021**, *129*, 107994. [CrossRef]
41. Cao, S.; Chen, L.; Yu, X. Impact of China's Grain for Green Project on the landscape of vulnerable arid and semi-arid agricultural regions: A case study in northern Shaanxi Province. *J. Appl. Ecol.* **2009**, *46*, 536–543. [CrossRef]
42. Yuan, W.; Li, X.; Liang, S.; Cui, X.; Dong, W.; Liu, S.; Xia, J.; Chen, Y.; Liu, D.; Zhu, W. Characterization of locations and extents of afforestation from the Grain for Green Project in China. *Remote Sens. Lett.* **2014**, *5*, 221–229. [CrossRef]
43. Bai, Y.; Yang, Y.; Jiang, H. Intercomparison of AVHRR GIMMS3g, terra MODIS, and SPOT-VGT NDVI products over the Mongolian plateau. *Remote Sens.* **2019**, *11*, 2030. [CrossRef]
44. Jiang, W.; Yuan, L.; Wang, W.; Cao, R.; Zhang, Y.; Shen, W. Spatio-temporal analysis of vegetation variation in the Yellow River Basin. *Ecol. Indic.* **2015**, *51*, 117–126. [CrossRef]
45. Tian, Y.; Bai, X.; Wang, S.; Qin, L.; Li, Y. Spatial-temporal changes of vegetation cover in Guizhou Province, Southern China. *Chinese Geogr. Sci.* **2017**, *27*, 25–38. [CrossRef]
46. Jin, K.; Wang, F.; Han, J.Q.; Shi, S.Y.; Ding, W.B. Contribution of climatic change and human activities to vegetation NDVI change over China during 1982—2015. *Acta Geogr. Sin.* **2020**, *75*, 961–974.
47. Gao, J.B.; Jiao, K.W.; Wu, S.H. Revealing the climatic impacts on spatial heterogeneity of NDVI in China during 1982—2013. *Acta Geogr. Sin.* **2019**, *74*, 534–543.